# Critical impact of Ehrlich-Schwöbel barrier on GaN surface morphology during homoepitaxial growth

Nils. A.K. Kaufmann[1], L. Lahourcade[1], B. Hourahine[2], D. Martin[1], and N. Grandjean[1]

[1] *Institute of Condensed Matter Physics, Ecole polytechnique fédérale de Lausanne (EPFL), CH-1015 Lausanne – Switzerland*

[2] *Department of Physics, SUPA, University of Strathclyde, John Anderson Building, 107 Rottenrow, Glasgow G4 0NG, United Kingdom*

We discuss the impact of kinetics, and in particular the effect of the Ehrlich-Schwöbel barrier (ESB), on the growth and surface morphology of homoepitaxial GaN layers. The presence of an ESB can lead to various self-assembled surface features, which strongly affect the surface roughness. We present an in-depth study of this phenomenon on GaN homoepitaxial layers grown by metal organic vapor phase epitaxy and molecular beam epitaxy. We show how a proper tuning of the growth parameters allows for the control of the surface morphology, independent of the growth technique.

## I. Introduction

III-nitride based optoelectronic devices, e.g. light emitting diodes (LEDs) and laser diodes (LDs), are nowadays widely commercialized. One of the key features of III-nitrides is the broad range of wavelengths over which their direct bandgap spans, covering the whole visible spectrum and even a large part of the UV spectral domain. However, the best optoelectronic device efficiency is obtained in the near UV and blue spectral ranges because of severe drawback when aiming at synthesizing heterostructures, due to the large lattice mismatches between GaN, AlN and InN. Furthermore, the different growth conditions required for the binary compounds makes the synthesis of high quality ternary or quaternary alloys very challenging. Despite substantial progress the past years, these material issues are still hindering the performance of short and long wavelength nitride optoelectronic devices. Another concern is the lack of large area GaN native single crystal substrates. Therefore GaN growth was initially developed on foreign substrates like SiC, sapphire, or even silicon. Despite huge threading dislocation densities associated with the large lattice mismatch between GaN and these substrates, high efficiency LEDs were successfully fabricated with dislocation densities of $10^8$ – $10^9$ $cm^{-2}$ [1]. However the fabrication of high performance LDs calls for the use of low dislocation density high quality GaN substrates to enhance the overall efficiency of InGaN quantum wells (QWs) [2]. In addition to the reduction of structural defects, the control of smooth surface and interface morphologies is also of prime importance. Indeed, beside interface roughness and alloy disorder, which both contribute to QW transition energy fluctuations, local surface misorientation has been shown to strongly influence the incorporation of indium in InGaN QWs.[3, 4]. This points out how important is the surface morphology of GaN homoepitaxial layers.

Smooth GaN layers grown in the step-flow mode [5] can be produced by both metal organic vapor phase epitaxy (MOVPE) and metal-rich plasma-assisted molecular beam epitaxy (PAMBE) [6, 7, 8, 9]. On the other hand, hexagonal hillock morphology has been reported for GaN grown either by ammonia MBE ($NH_3$-MBE) [7, 10] or nitrogen-rich PAMBE [8, 9]. In the case of $NH_3$-MBE, the formation of these hillocks is not induced by surface defects like threading dislocations propagating through the whole layer and terminating at the surface to induce spiral growth. Instead it is ascribed to kinetic effects which may originate from the presence of an Ehrlich-Schwöbel barrier (ESB) [7, 10]. The ESB is an energy barrier located at step-edges, which adatoms need to overcome to diffuse down the step and attach to the lower step-edge [11, 12]. In the presence of such a barrier, the probabilities of attachment to the upper and lower step-edges are different. This asymmetry makes the growth unstable against any perturbation in height. As a consequence, it induces an uphill mass-current which, in turn, can induce specific self-assembled surface features [13, 14]. The effects of an ESB on layer morphology have been observed in many materials grown at low temperatures [14-17], and in particular in GaN layers [18]. Thus ESB may have critical consequences for the fabrication of high indium content InGaN-based optoelectronic devices where the growth temperature of the GaN barriers cannot be much higher than that of the InGaN QWs in order to avoid both indium desorption and InGaN alloy degradation [19 - 22].

In this paper, we will first investigate the effect of an ESB on GaN layers depending on growth conditions and growth techniques. Our experimental findings will be compared to kinetic Monte Carlo (KMC) simulations. We will demonstrate that various kinds of surface morphology can be obtained by tuning the growth conditions, independently of the growth technique.

Figure 1 illustrates the modification of the nucleation processes in the step-flow growth mode regime induced by the presence of an ESB. While in the standard step-flow regime the adatoms attach to both the downward or upward step-edges (Fig. 1(a)), the ESB hinders the incorporation at the downward step-edge (Fig. 1(b)). Actually the nucleation of the adatoms depends on $\Lambda/L$, where $\Lambda$ is their diffusion length (defined on a step-free surface) and $L$ the mean step-edge distance (mean step width). One dimensional (1D) nucleation occurs when the nucleation takes place at the step-edges, *i.e.* for $\Lambda >> L$. When reducing $\Lambda$ for a given step-width, two-dimensional islands may start to form on the steps (2D nucleation). In the absence of an ESB, initial island nucleation statistically takes place at the center of the steps (Fig. 1(c)). On the other hand, in the presence of an ESB, islands start to nucleate closer to the downward step-edge due to an increase of the local adatom density (Fig. 1(d)). Eventually, this induces a transition from 1D to 2D nucleation as well, but for larger diffusion lengths [18].

## II. Experiment

For this study, *c*-plane layers were grown either on standard GaN-on-sapphire templates or on free-standing (FS) GaN substrates. We deliberately focused on homoepitaxial growth of GaN to get rid of the influence of strain. The GaN-on-sapphire templates were fabricated by MOVPE at high temperature (1050°C). We used as well FS substrates to minimize the effect of dislocations. Note that the surface misorientation is in the range of 0.3 to 0.5° whatever the substrate. Low temperature MOVPE GaN layers were deposited at around 840°C with $N_2$ as carrier gas, which corresponds to typical conditions used for the growth of InGaN/GaN QWs. In the case of $NH_3$-MBE, the layers were grown between 800°C and 920°C. Finally, PAMBE layers were deposited under either Ga-rich conditions at 740°C or nitrogen-rich conditions at

790°C, using the growth window described by Koblmueller *et al.* [22, 23]. Atomic force microscopy (AFM) was used to characterize the surface morphology of the samples and determine the growth modes.

## III. Modelling

Two dimensional Kinetic Monte Carlo simulations of growth modes were also performed. Following the *minimal* model of ref. [24], the growth process is represented as the deposition of units of type B which are eventually converted to the crystal material, which is composed of units of type A. Both types of unit are capable of diffusion on the surface with a small barrier. The less mobile A units experience an additional barrier to motion proportional to the number of their neighbors in the same bilayer or above (as occurs at upward steps). Only units of type B experience the ESB at step edges, and will convert to A units either spontaneously or at upward step edges of the substrate. To accommodate the double bilayer structure of the wurtzite lattice along [0001], sites for only one sub-lattice on alternating bilayers are considered in the simulation (Fig. 2), this leads to a small offset in the simulation grids between the two types of bilayer along the [11-20] direction. The simulations were performed to deposit 1000 monolayers (MLs) of material onto the substrate, at rates of between 1 and 80 ML/s, and for both 400 x 400 and 800 x 800 site models with screw periodic boundary conditions. Diffusion prefactors of $10^{12}$ – $10^{14}$ $s^{-1}$ were considered, with surface diffusion barriers of 1.0 eV for both A and B species. In addition, the barrier for B diffusion was increased by 0.3 eV for each of its neighbors at the same height or above. The ESB was set to be 1.0 eV and the barrier for spontaneous conversion of A to B was 1.173 eV.

## IV. Surface morphology of GaN epilayers

The ESB-induced adatom nucleation has a profound impact on the surface morphology of growing layers, which can be classified within three different categories namely hillock, step-meandering, or step-bunching [13, 14, 24]. Hillock formation was first theoretically described by Villain [25, 26]. It occurs in the 2D island nucleation regime, *i.e.* on flat surfaces or when the off-axis crystal misorientation is small (meaning relatively large steps). For instance, this growth regime has been observed for germanium homoepitaxially grown at low temperature [15]. In the case of larger offcut angles, for which the nucleation mainly takes place at the step-edges, step-meandering prevails. The surface morphology is then characterized by valleys running perpendicularly to the step-edges. See for example meandering in Cu [16] or Si [17] growth. This specific growth instability develops in the presence of an ESB at a step-edge, which is referred to as the step Ehrlich-Schwöbel effect (SESE) [27], but also when the ESB is located at a kink along the step-edge. In this case, it is referred to as kink Ehrlich-Schwöbel effect (KESE) [13, 14].

Due to the specific step-edge atomic bond configuration imposed by the wurtzite structure, (0001) GaN surfaces exhibit stable steps of two ML height [28]. Note that the role of the ESB on macro steps (*i.e.* 4 ML or more) [29] will not be treated here. Both hillock and step-meandering regimes occur in the case of GaN. This is illustrated by AFM images of GaN homoepitaxial layers in Figs. 3(a) and 3(b), for growth at 800°C by $NH_3$-MBE and at 840°C by MOVPE, respectively. For comparison, Fig. 3(c) displays a typical AFM image of a GaN film deposited by MOVPE under “standard” high temperature growth conditions (1050°C, $H_2$ as carrier gas), for which step-flow mode takes place. In order to verify the kinetic origin of these surface morphologies, the samples were annealed at 1000°C under $NH_3$ atmosphere. As expected all annealed samples display regular staircase surface features similar to what is

observed in Fig. 3(c). KMC simulations carried out including ESB effects on a hexagonal system are displayed in Fig. 3 as well: when increasing the diffusion length, the surface is predicted to evolve from hillocks to step-meandering (Figs. 3(d) and (e), respectively). Step-flow-like surface is obtained when considering a very low (or no ESB) (Fig. 3(f)). These simulations are in line with our experimental results and consistent with previous KMC simulations developed for a cubic system [24]. This further confirms the kinetic origin of the different surface morphologies.

As already mentioned, the surface morphology is governed by $\Lambda/L$, and the growth temperature ($T_{gr}$) is the main parameter that affects $\Lambda$. As an illustration, the surface morphologies of a GaN homoepitaxial layers grown by $NH_3$-MBE at three different temperatures are displayed in Fig. 4: hillocks are observed for $T_{gr}$ = 800°C (Fig. 4(a)) and step-meandering for $T_{gr}$ = 865°C (Fig. 4(b)). The high decomposition rate of GaN at high temperature [30] requires a large $NH_3$ overpressure, which rapidly becomes incompatible with molecular beam requirements. Thus we were limited to a temperature of 920°C, for which the surface gets smoother (Fig. 4(c)) but not as smooth as surfaces obtained with MOVPE at $T_{gr}$ > 1000°C. When increasing $T_{gr}$ over this range of temperatures, the root mean square surface roughness for a 5 x 5 µm² area reduces from 6.1 to 1.1 nm.

These three different surface morphologies have also been reproduced using PAMBE, for which it is well known that smooth GaN surfaces can be obtained (Fig. 4(f)) under properly tuned gallium-rich conditions [31]. On the other hand, when decreasing the III/V ratio towards nitrogen-rich conditions, 3D hillock morphology is often observed [32]. However, at higher growth temperature and using the growth window described by Koblmueller *et al.* [22, 23], both hillock and step-meandering can form under nitrogen-rich conditions, as illustrated in Figs. 4(d) and (e). In these particular cases, a sample was grown at 790°C, but with different surface misorientations due to local variations of the miscut angle of FS GaN substrate, which in turn induce various $\Lambda/L$ values, hence different growth modes.

**V. Scaling of the surface morphology**

First of all, it should be mentioned that an excess of endogeneous or exogeneous adatoms at the surface can induce a surfactant effect [33], which will modify the diffusion length $\Lambda$ and thus the surface morphology. Here we intentionally did not consider those situations when investigating the scaling behavior of GaN growth.

As shown in Fig. 5(a) for hillocks, the height of the features increases slowly with the thickness of the layer, while their lateral dimension remains constant. This is characteristic of ESB-induced surface roughening [13]. However this holds only for homoepitaxial growth. In the case of heteroepitaxy, the lateral dimensions might change due to strain relaxation processes, leading to thickness-dependent feature sizes [10]. Theoretically, for a given growth temperature, the lateral feature size ($\lambda$) (or periodicity) should be proportional to $V_{gr}^{-\beta}$, with $V_{gr}$ the growth rate and $\beta$ the scaling factor [13, 34]. Indeed, the growth rate affects the mean-free path of the adatoms and therefore their effective diffusion length. In Fig. 5(b), $\lambda$ is plotted over $V_{gr}$ for both the hillock and the step-meandering regimes (see the corresponding AFM images in the insets). From these plots, we extracted scaling factors of 0.61 and 0.45, respectively. As expected, $\beta$ is larger for hillock regime than for step-meandering. This comes from the fact that, in the hillock regime, the mass transport contributing to surface

modulations comes laterally from all directions, whereas only the mass transport parallel to the steps contributes in the step-meandering regime. In the literature, one can find $\beta$ ~ 0.5 for 2D SESE and $\beta$ ~ 0.25 for 1D KESE (both for step-meandering) [34-36]. In our study, $\beta$ = 0.45 is close to the theoretical value of 0.5 and is therefore in favor of a dominant 2D SESE. Here, one should notice that this scaling law remains valid within one growth regime only. Indeed, by reducing the growth rate and thereby increasing the diffusion length, nucleation processes can change from 2D to 1D. On the other hand, a transition from step-meandering to smooth step-flow morphology may occur by further reducing the growth rate (dashed line in Fig. 5(b)). This will be discussed in more detail in the following.

## VI. Control of the surface morphology and growth conditions

Various strategies can be implemented to get rid of ESB-induced surface roughness:

(i) to use high growth temperature, in order to provide enough thermal activation energy to the adatoms to overcome the ESB. This corresponds to standard MOVPE growth conditions, with $T_{gr}$ > 1000°C (Fig. 3(c)). However, high $T_{gr}$ cannot always be sustained, especially for high indium content InGaN and InAlN alloys.

(ii) to use a low growth rate when growing at low temperatures. This way, smoothening effects such as desorption [13] can become dominant and eventually counter the ESB-induced uphill mass-current. As mentioned earlier, a transition from step-meandering to step-flow growth mode is observed when reducing the growth rate. The decreased number of adatoms leads to a fast drop of the ESB-induced uphill mass-current. Additionally, a countering downhill mass-current can reduce and even annihilate the ESB, preventing the formation of surface modulations. This downhill mass-current can for instance come from a curvature-dependent desorption. Thus step-flow growth could theoretically still occur in the presence of an ESB. However, the very low growth rates required for this transition make it less suitable from a technology point of view.

(iii) to create an alternative diffusion channel, so that adatoms no longer experience the ESB. This is the case of Ga-rich PAMBE conditions for which smooth surfaces are achieved at low growth temperature when a Ga-bilayer is stabilized at the growth front. It was proposed that the presence of the metal adlayer leads to the creation of an additional diffusion channel on the step, leading to enhanced surface diffusion [37]. However, a better understanding of the role of Ga adatoms on the surface morphology is provided by the STM study of the island nucleation processes by Zheng *et al.* [18]. As schematically illustrated in Fig. 6(a), without metal adlayer the ESB prevails and the initial island nucleation takes place close to the downward step, as already explained. With a single layer of Ga in excess at the growth front, one may infer that the ESB is screened for single-steps (Fig. 6(b)) but not double-steps Fig. 6(c): the ESB might be screened if the metal adlayer is sufficiently thick to provide a continuous layer over the step-edge (Fig. 6(d)). As mentioned earlier, GaN (0001) surfaces exhibit double steps [28], thus the screening of the ESB requires a bilayer of metal [8, 9]. It should be stressed that it is not the metal-enhanced diffusion on the steps, as proposed at first, but the screening of the ESB at the step-edges which enables getting smooth GaN surface at low temperatures. Note that for other GaN crystal planes, different optimum metal film thicknesses were reported (e.g. a trilayer of Ga for *m*-plane GaN [38]).

iv) to change the surface chemistry. In the case of MOVPE, the carrier gas is a crucial growth parameter. For instance, GaN grown using $H_2$ as carrier gas exhibits a smooth surface morphology, whether it is deposited at high temperature (Fig. 7(a)) or low temperature (Fig.

7(b)). On the other hand, step-meandering is observed on GaN grown at low temperature with $N_2$ as carrier gas, (Fig. 7(c)). One can invoke two possible effects of hydrogen at surface: either it enhances the smoothing effects (by self-etching of the growth front), or it promotes the formation of a partial metal adlayer at the growing surface [39].

The different growth windows for GaN homoepitaxy deduced from this work are summarized in Fig.8. As discussed before, the presence of an ESB affects the nucleation behavior and shifts the transition between nucleation on the steps (Fig. 1(c)) and nucleation only at the step-edges (Fig. 1(d)). For identical step-width, the island nucleation on the steps starts for higher diffusion length when an ESB is present (Fig. 8(a)). For a given surface misorientation, the ratio can be controlled by both the growth rate and temperature. Therefore, we summarize the different surface morphologies induced by an ESB as function of the growth parameters (Fig. 8(b)). This growth phase diagram applies for both MOVPE and MBE, as long as the ESB is not screened by specific surface chemistry.

## VII. Summary

The surface morphology of GaN homoepitaxial layers has been studied for various growth conditions. The Ehrlich-Schwöbel energy barrier at the step-edges makes the growth unstable at low temperatures. It induces surface features like hillocks or step-meandering, depending of the growth parameters. The scaling behavior of these surface modulations is consistent with theoretical models describing ESB-induced surface roughening. We confirmed that the surface features of GaN layers grown by either MBE or MOVPE directly depend on the growth conditions but not on the growth technique itself. We also stress that ESB-induced surface roughening may significantly impact the subsequent growth of InGaN layers due to the indium incorporation dependence on step-edge density. Also the ESB even affects the InGaN growth itself. Smooth surfaces can however be obtained at low temperature providing the screening of the ESB. This is the case for instance of PAMBE growth when a Ga-bilayer is present on the growing surface. Finally it should be mentioned that the ESB phenomenon is likely to play a role for other III-nitride materials too. For instance, hillock morphology was also observed for InGaN [3], InAlN [40], AlGaN, AlN [41] and InN [42], and step-meandering for InGaN [43]. In turn, growth front roughening should strongly impact the incorporation of various species [4, 21, 22, 44, 45]. These results point out the huge effect of the ESB on III-nitride polar semiconductor growth

## VIII. Acknowledgements

This work was partly supported by EU-project ITN Rainbow (Grant No. PITN-GA-2008-213238).

**Figure 1:**

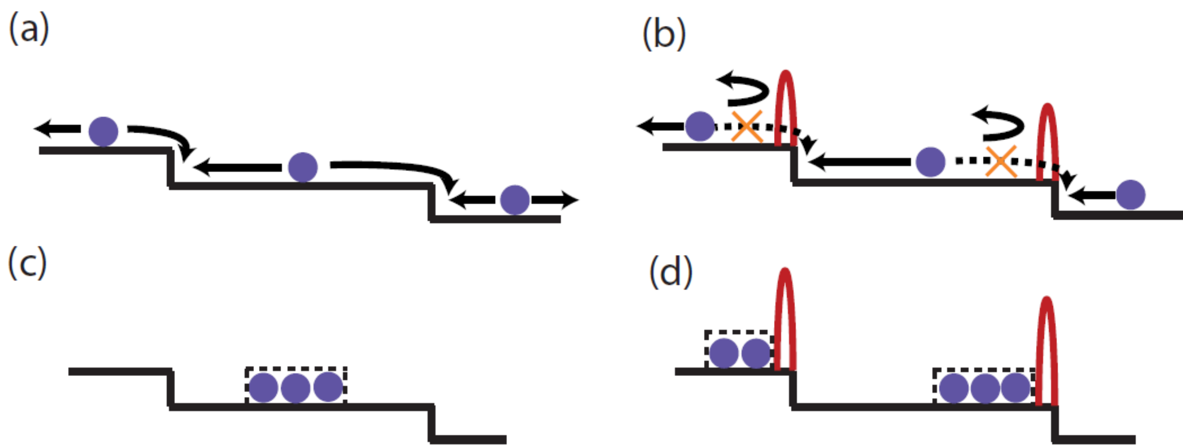


Schematic of step-flow growth mode without (a) and with (b) an ESB. Nucleation on the terrace of 2D islands without (c) and with (d) an ESB.

**Figure 2:**

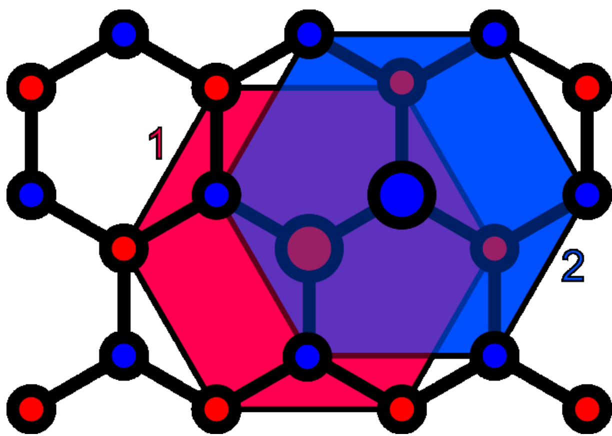


Neighbors of atomic sites in the kinetic Monte Carlo simulations. The sub-lattices and six site neighbors for a site (larger circle) in each of the two bilayers, 1 and 2, are shown in red and blue respectively. Only one physical sublattice is represented in the simulations, with a displacement of the hexagonal grid along ± [11-20] between each bilayer.

**Figure 3:**

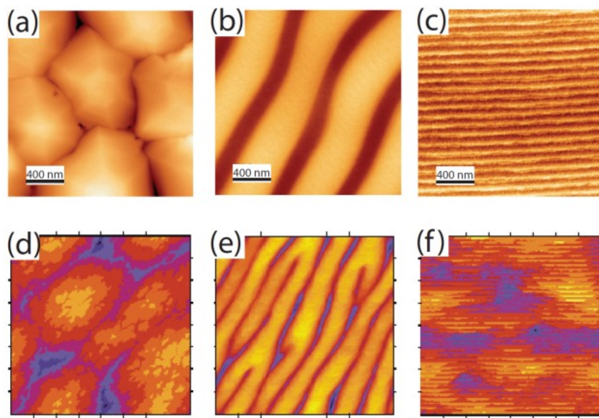


AFM images of GaN epilayers and corresponding KMC simulation images for (a) and (d) the hillock regime, (b) and (e) the step-meandering regime, (c) and (f) the step-flow regime. The layer in (a) was grown by $NH_3$-MBE at 800°C. The layers in (b) and (c) were grown by MOVPE at 840°C and 1050°C, respectively.

**Figure 4:**

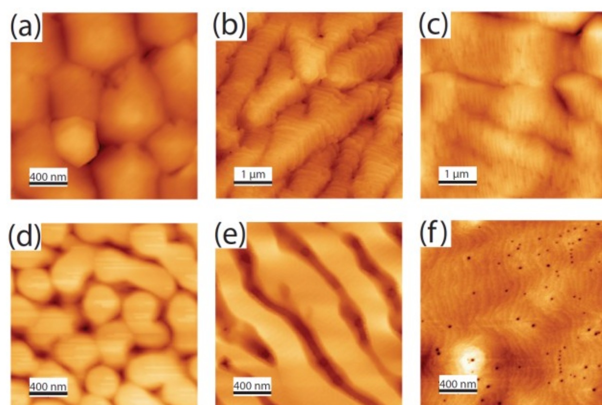


AFM images of $NH_3$-MBE-grown GaN layers in hillock, step-meandering, and step-flow regime. For (a), (b) and (c) the growth temperatures were 800°C, 865°C and 920°C, respectively. The sample displayed in (d) and (e) was grown by nitrogen-rich PAMBE at 790°C on FS GaN (unintentionally offcut variations of the GaN FS substrate are responsible for the different morphologies). (f) Step-flow growth surface obtained by PAMBE at 740°C under metal-rich conditions.

**Figure 5:**

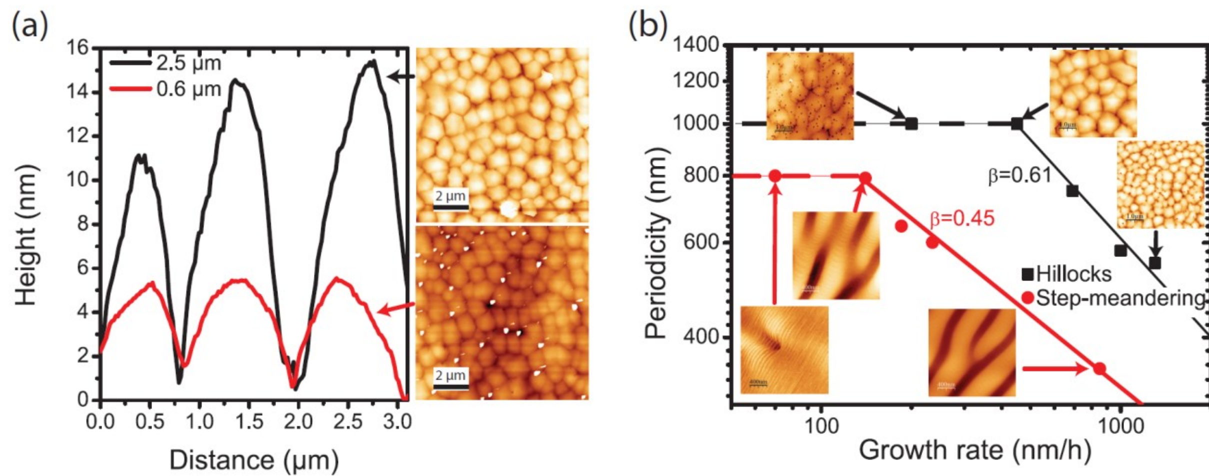


(a) Dependence of the peak-to-valley ratio with the layer thickness. (b) Dependence of the periodicity $\lambda$ with the growth rate $V_{gr}$ for the hillock regime (black) and the step-meandering regime (red), for layers grown by $NH_3$-MBE and MOVPE, respectively. A scaling factor of $\beta$ = 0.61 is deduced for the hillock morphology and $\beta$ = 0.45 for the step-meandering regime. At very low $V_{gr}$ a transition between two different growth regimes occurs, indicated by the dashed lines.

**Figure 6:**

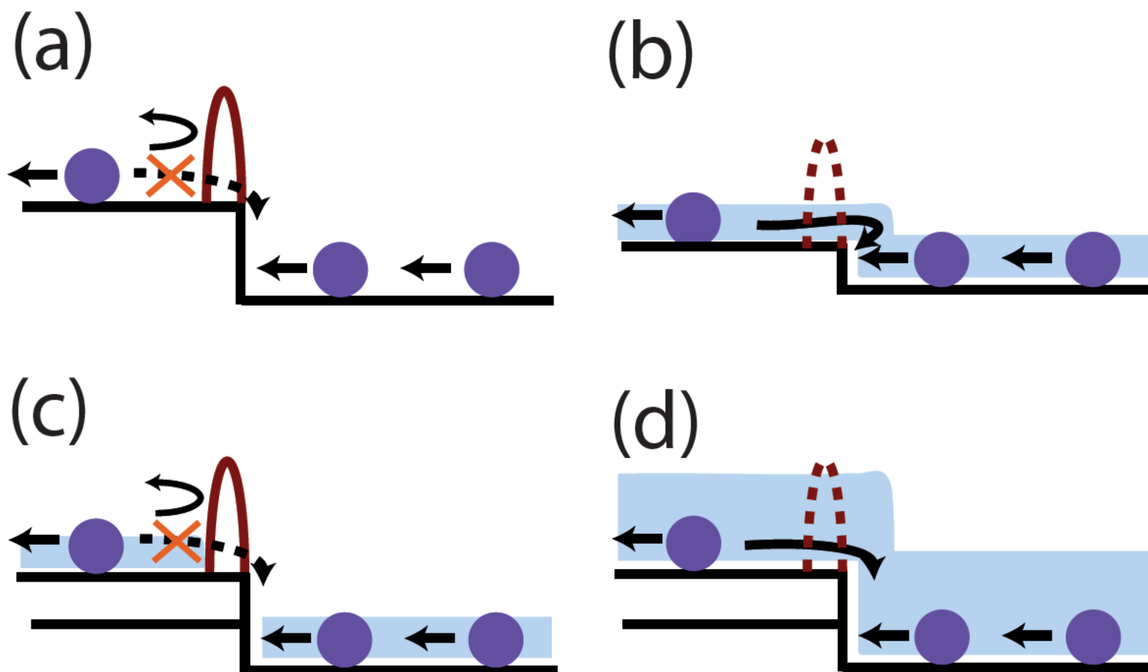


Schematic of the effect of Ga-metal adlayers during growth on GaN surface. (a) Reference case where the ESB is at play. A monolayer-thick Ga adlayer allows for (b) the screening of the ESB for single steps but (c) is not sufficient for double steps. (d) A continuous Ga bilayer allows for the screening of the ESB for double steps (PAMBE growth conditions).

**Figure 7:**

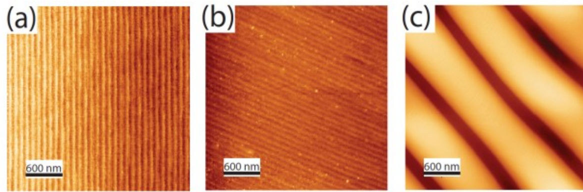


AFM images of GaN layers grown by MOVPE with $H_2$ as carrier gas at (a) 1050°C and (b) 840°C and (c) with $N_2$ as carrier gas at 840°C.

**Figure 8:**

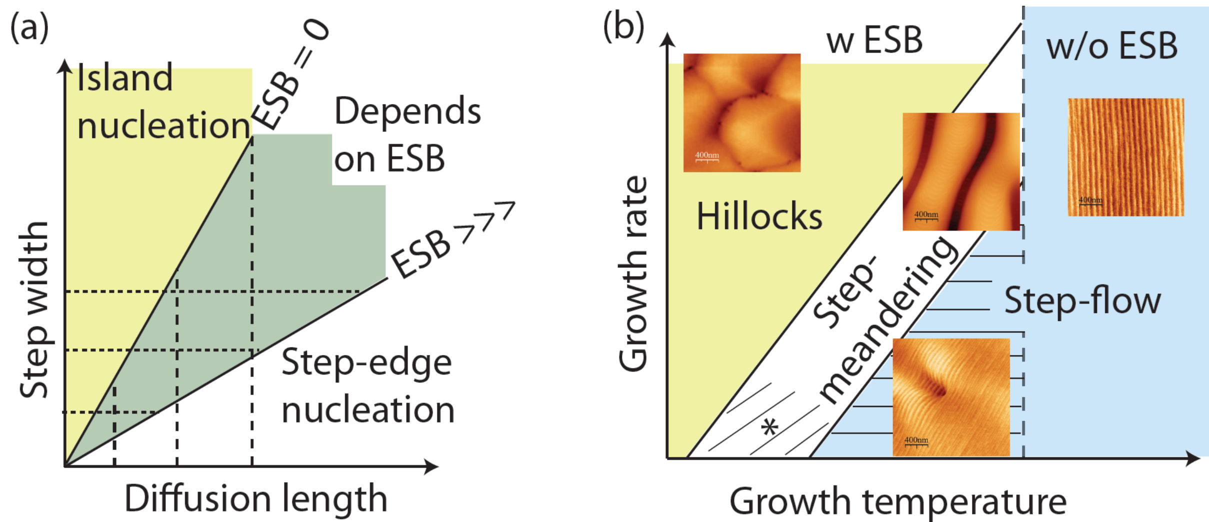


(a) Schematic of the transition between island nucleation and step-edge nucleation as a function of step width and diffusion length, with and without an ESB. (b) Phase diagram of the different growth regimes (assuming a fixed misorientation) as a function of the growth rate and temperature. Horizontal lines indicate a regime where smoothening effects dominate, allowing for step-flow growth despite the presence of an ESB. The star-marked area corresponds to conditions for which step-bunching is expected to occur. At high growth temperature the effects of the ESB can be neglected.

References:


[1] S. D. Lester, F. A. Ponce, M. G. Craford and D. A. Steigerwald, *High dislocation densities in high efficiency GaN-based light-emitting diodes*, Appl. Phys. Lett. **66**, 1249 (1995)

[2] S. Nakamura, M. Senoh, S. Nagahama, N. Iwasa, T. Yamada, T. Matsushita, H. Kiyoku, Y. Sugimoto, T. Kozaki, H. Umemoto, M. Sano and K. Chocho, *Continuous-wave operation of InGaN/GaN/AlGaN-based laser diodes grown on GaN substrates*, Appl. Phys. Lett. **72**, 2014 (1998)

[3] M. Sarzynski, M. Leszczynski, M. Krysko, J.Z. Domagala, R. Czernecki and T. Suski, *Influence of GaN substrate off-cut on properties of InGaN and AlGaN layers*, Chrys. Res. and Tech. **47**, 321 (2012)

[4] T. Lermer, I. Pietzonka, A. Avramescu, G. Bruederl, J. Mueller, S. Lutgen and U. Strauss, *Interdependency of surface morphology and wavelength fluctuations of indium-rich InGaN/GaN quantum wells*, Phys. Stat. Sol. A **208**, 1199 (2011)

[5] W. K. Burton, N. Cabrera and F. C. Frank, *The growth of crystals and the equilibrium structures* of their surfaces, Philosophical Transactions of the royal society of London Series A **243**, 299 (1951)

[6] B. Heying, E. J. Tarsa, C. R. Elsass, P. Fini, S. P. DenBaars, J. S. Speck, *Dislocation mediated surface morphology of GaN*, J. of Appl. Phys. **85**, 6470 (1999)

[7] A. L. Corrion, F. Wu and J. S. Speck, *Growth regimes during homoepitaxial growth of GaN by ammonia molecular beam epitaxy*, J. Appl. Phys. **112**, 054903 (2012)

[8] C. Adelmann, J. Brault, D. Jalabert, P. Gentile, H. Mariette, G. Mula and B. Daudin, *Dynamically stable gallium surface coverages during plasma-assisted molecular-beam epitaxy of (0001)GaN*, J. App. Phys. **91**, 9638 (2002)

[9] G. Koblmueller, J. Brown, R. Averbeck, H. Riechert, P. Pongratz and J.S. Speck, *Ga adlayer governed surface defect evolution of (0001)GaN films grown by plasma-assisted molecular beam epitaxy*, Jap. J. Appl. Phys. **44**, L906 (2005)

[10] S. Vezian, F. Natali, F. Semond and J. Massies, *From spiral growth to kinetic roughening in molecular-beam epitaxy of GaN(0001)*, Phys. Rev. B **69**, 125329 (2004)

[11] G. Ehrlich and F.G. Hudda, *Atomic view of surface self-diffusion - tungsten on tungsten*, J. Chem. Phys. **44**, 1039 (1966)

[12] R.L. Schwoebel and E.J. Shipsey, *Step motion on crystal surfaces*, J. Appl. Phys. **37**, 3682 (1966)

[13] C. Misbah, O. Pierre-Louis and Y. Saito, *Crystal surfaces in and out of equilibrium: A modern view*, Rev. Mod. Phys. **82**, 981 (2010)

[14] P. Politi, G. Grenet, A. Marty, A. Ponchet and J. Villain, *Instabilities in crystal growth by atomic or molecular beams*, Phys. Lett. **324**, 271 (2000), J. Krug, *Kinetic pattern formation at solid surfaces*, in G. Radons, W. Just and P.Haussler, *Collective Dynamics of non linear and disordered systems*, 5–37, WE Heraeus Fdn (Springer-Verlag Berlin, Germany (2005), O. Pierre-Louis, M.R. D'Orsogna and T.L. Einstein,

*Edge Diffusion during Growth: The Kink Ehrlich-Schwoebel Effect and Resulting Instabilities*, Phys. Rev. Lett. **82**, 3661 (1999)

[15] K. A. Bratland, Y. L. Foo, J. A. N. T. Soares, T. Spila, P. Desjardins and J. E. Greene, *Mechanism for epitaxial breakdown during low-temperature Ge(001) molecular beam epitaxy*, Phys. Rev. B **67**, 125322 (2003)

[16] T. Maroutian, L. Douillard and H.J. Ernst, *Morphological instability of Cu vicinal surfaces during step-flow growth*, Phys. Rev. B **64**, 165401 (2001)

[17] H. Omi and T. Ogino, *Growth-induced atomic step ordering on patterned and non-patterned Si(111)*, Thin Solid Films **380**, 15 (2000), R.T. Tung and F. Schrey, *Topography of the Si(111) surface during silicon molecular-beam epitaxy*, Phys. Rev. Lett. **63**, 1277 (1989), N. Galiana, P. P. Martin, C. Munuera, M. Varela, C. Ocal, M. Alonso and A. Ruiz, *Pyramid-like nanostructures created by Si homoepitaxy on Si(001)*, Material Science In Semiconductor Processing **12**, 52 (2009)

[18] H. Zheng, M. H. Xie, H. S. Wu and Q. K. Xue, *Kinetic energy barriers on the GaN(0001) surface: A nucleation study by scanning tunneling microscopy*, Phys. Rev. B **77**, 045303 (2008)

[19] U. Strauss, A. Avramescu, T. Lermer, D. Queren, A. Gomez-Iglesias, C. Eichler, J. Mueller, G. Bruederl and S. Lutgen, *Pros and cons of green InGaN laser on c-plane GaN*, Phys. Stat. Sol. B **248**, 652 (2011)

[20] D. Queren, M. Schillgalies, A. Avramescu, G. Bruederl, A. Laubsch, S. Lutgen and U. Strauss, *Quality and thermal stability of thin InGaN films*, J. Cryst. Growth **311**, 2933 (2009)

[21] S.M. Olaizola, S. T. Pendlebury, J. P. O'Neill, D. J. Mowbray, A. G. Cullis, M. S. Skolnick, P. J. Parbrook and A. M. Fox, *Influence of GaN barrier growth temperature on the photoluminescence of InGaN/GaN heterostructures*, J. Phys. D: Appl. Phys. **35**, 1-5 (2002)

[22] D. D. Koleske, S. R. Lee, M. H. Crawford, K. C. Cross, M. E. Coltrin and J. M. Kempisty, *Connection between GaN and InGaN growth mechanisms and surface morphology*, J. Cryst. Growth **391**, 84-96 (2013)

[22] G. Koblmueller, F. Wu, T. Mates, J. S. Speck, S. Fernandez-Garrido and E. Calleja, *High electron mobility GaN grown under N-rich conditions by plasma-assisted molecular beam epitaxy*, Appl. Phys. Lett. **91**, 221905 (2007)

[23] G. Koblmueller, F. Reurings, F. Tuomisto and J. S. Speck, *Influence of Ga/N ratio on morphology, vacancies, and electrical transport in GaN grown by molecular beam epitaxy at high temperature*, Appl. Phys. Lett. **97**, 191915 (2010)

[24] M. Vladimirova, A. Pimpinelli and A. Videcoq, *A new model of morphological instabilities during epitaxial growth: from step bunching to mounds formation*, J. Crys. Growth **220**, 631 (2000)

[25] J. Villain, *Continuum models of crystal-growth from atomic-beams with and without desorption*, J. de Physique I **1**, 19 (1991),

[26] P. Politi and J. Villain, *Ehrlich-Schwoebel instability in molecular-beam epitaxy: A minimal model*, Phys. Rev. B **54**, 5114 (1996)

[27] G.S. Bales, A. Zangwill, *Morphological instability of a terrace edge during step-flow growth*, Phys. Rev. B **41**, 5500 (1990)

[28] M.H. Xie, S.M. Seutter, W.K. Zhu, L.X. Zheng, H.S. Wu and S.Y. Tong, *Anisotropic step-flow growth and island growth of GaN(0001) by molecular beam epitaxy*, Phys. Rev. Let. **82**, 2749 (1999)

[29] M.G. Lagally and Z.Y. Zhang, *Materials science - Thin-film cliffhanger*, NATURE **417**, 907 (2002)

[30] N. Grandjean, J. Massies, F. Semond, S. Yu. Karpov and R. A. Talalaev, *GaN evaporation in molecular beam epitaxy environment*, Appl. Phys. Lett. **74**, 1854 (1999)

[31] B. Heying, R. Averbeck, L. F. Chen, E. Haus, H. Riechert and J. S. Speck, *Control of GaN surface morphologies using plasma-assisted molecular beam epitaxy*, J. Appl. Phys. **88**, 1855 (2000)

[32] C. Skierbiszewski, M. Siekacz, P. Perlin, A. Feduniewicz-Zmuda, G. Cywinski, I. Grzegory, M. Leszczyniski, Z. R. Wasilewski and S. Porowski, *Role of dislocation-free GaN substrates in the growth of indium containing optoelectronic structures by plasma-assisted MBE*, J. Cryst. Growth **305**, 346 (2007)

[33] J. Massies and N. Grandjean, *Surfactant effect on the surface-diffusion length in epitaxial growth*, Phys. Rev. B **48**, 8502 (1993)

[34] M. Rusanen, I.T. Koponen, J. Heinonen and T. Ala-Nissila, *Instability and wavelength selection during step flow growth of metal surfaces vicinal to fcc(001)*, Phys. Rev. Lett. **86**, 5317 (2001)

[35] T. Maroutian, L. Douillard and H.J. Ernst, *Wavelength selection in unstable homoepitaxial step flow growth*, Phys. Rev. Lett. **83**, 4353 (1999)

[36] J. Krug, *On the shape of wedding cakes*, J. Stat. Phys. **87**, 505 (1997)

[37] J. Neugebauer, T.K. Zywietz, M. Scheffler, J.E. Northrup, H. Chen and R.M. Feenstra, *Adatom Kinetics On and Below the Surface: The Existence of a New Diffusion Channel*, Phys. Rev.Lett. **90**, 056101 (2003)

[38] O. Brandt, Y.J. Sun, L. Daweritz and K.H. Ploog, *Ga adsorption and desorption kinetics on M-plane GaN*, Phys. Rev. B **69**, 165326 (2004)

[39] E.V. Yakovlev, R.A. Talalaev, A.S. Segal, A.V. Lobanova, W.V. Lundin, E.E. Zavarin, M.A. Sinitsyn, A.F. Tsatsulnikov and A.E. Nikolaev, *Hydrogen effects in III-nitride MOVPE*, J. Cryst. Growth 310, 4862 (2008)

[40] G. Perillat-Merceroz, G. Cosendey, J.F. Carlin, R. Butte, N. Grandjean, *Intrinsic degradation mechanism of nearly lattice-matched InAlN layers grown on GaN substrates*, J. Appl. Phys. **113**, 063506 (2013)

[41] A. Matsuse, N. Grandjean, B. Damilano and J. Massies, *Surface morphology of AlN and size dispersion of GaN quantum dots*, J. Cryst. Growth **274**, 387 (2005)

[42] M. Himmerlich, S. Krischok, V. Lebedev, O. Ambacher and J.A. Schaefer, *Morphology and surface electronic structure of MBE grown InN*, J. Cryst. Growth **306**, 6 (2007)

[43] S. Sonderegger, E. Feltin, M. Merano, A. Crottini, J. F. Carlin, R. Sachot, B. Deveaud, N. Grandjean and J. D. Ganiere, *High spatial resolution picosecond cathodoluminescence of InGaN quantum wells*, Appl. Phys. Lett. **89**, 232109 (2006)

[44] M. Sawicka, A. Feduniewicz-Zmuda, H. Turski, M. Siekacz, S. Grzanka, M. Krysko, I. Dziecielewski, I. Grzegory and C. Skierbiszewski, *High quality m-plane GaN grown under nitrogen-rich conditions by plasma assisted molecular beam epitaxy*, J. Vac. Science & Tech. B **29**, 03C135 (2011)

[45] M. Funato, Y. S. Kim, T. Hira, A. Kaneta, Y. Kawakami, T. Miyoshi and S Nagahama, *Remarkably suppressed luminescence inhomogeneity in a (0001) InGaN green laser structure*, Appl. Phys. Express **6**, 111002 (2013)